

Gravity theories, Transverse Doppler and Gravitational Redshifts in Galaxy Clusters

HongSheng Zhao,¹ John A. Peacock,² and Baojiu Li³

¹*Scottish University Physics Alliance, University of St Andrews, KY16 9SS, UK*

²*Scottish University Physics Alliance, University of Edinburgh, EH9 3HJ, UK*

³*Institute of Computational Cosmology, Department of Physics, Durham University, Durham DH1 3LE, UK*

(Dated: 1.1.2012; Email address: hz4@st-andrew.ac.uk)

There is growing interest in testing alternative gravity theories using the subtle gravitational redshifts in clusters of galaxies. However, current models all neglect a transverse Doppler redshift of similar magnitude, and some models are not self-consistent. An equilibrium model would fix the gravitational and transverse Doppler velocity shifts to be about $6\sigma^2/c$ and $3\sigma^2/2c$ in order to fit the observed velocity dispersion σ self-consistently. This result comes from the Virial Theorem for a spherical isotropic cluster, and is insensitive to the theory of gravity. A gravitational redshift signal also does not directly distinguish between the Einsteinian and $f(R)$ gravity theories, because each theory requires different dark halo mass function to keep the clusters in equilibrium. When this constraint is imposed, the gravitational redshift has no sensitivity to theory. **Indeed our N-body simulations show that the halo mass function differs in $f(R)$, and that the transverse Doppler effect is stronger than analytically predicted due to non-equilibrium.**

PACS numbers: 98.10.+z, 95.35.+d, 98.62.Dm, 95.30.Sf

The theory of gravity has been subjected to various tests with the ever-improving quality of data from cosmology, galaxy clusters, galaxies and the solar system [1]. As shown by recent numerical N-body simulations on $f(R)$ type or scale-coupled gravities [2], dynamical data on non-linear cluster scales help to break theoretical degeneracies on linear cosmological scales, and overcome statistical uncertainties in observations. Past techniques often proposed comparing lensing data and kinematic data with simulations [3], which can involve significant amounts of effort in modeling of the mass distribution before indirect constraints can be set on the gravitational potential $\Phi(r)$ of the cluster. It would clearly be better to measure the gravitational potential in a galaxy cluster directly and compare this potential with the prediction from the Poisson equation for the mass distribution in a given gravity theory.

Indeed the gravitational potential is an observable from the shift of spectral lines [4]. Lines from the surface of the Sun, e.g., are shifted by $GM_\odot/R_\odot c \simeq 0.6 \text{ km s}^{-1}$, and more for compact stars. On cosmic scales, the deepest potential well $\Phi(r)$ is felt by the bright central galaxy (BCG) in a cluster of galaxies, where a nearly spherical distribution of many hundreds of galaxies orbit around the centre, with a Gaussian dispersion of random velocities of $\sigma(r) \sim 1000 \text{ km s}^{-1}$ in each direction. The observed line-of-sight Doppler shifts of galaxies relative to the BCG satisfy a Gaussian distribution with a small but non-zero mean velocity. This is partly due to the gravitational redshift (GR), a feature in any metric theory of gravity, caused by the spatial variation of the gravitational potential:

$$\Delta_{\text{GR}} = [\Phi_{\text{BCG}} - \Phi(r)]/c. \quad (1)$$

This signal of $\sim 10 \text{ km s}^{-1}$ becomes detectable above the σ/\sqrt{N} uncertainty of the mean velocity once the sample size $N \geq 10^4$. To obtain such a large sample for the first time, Wojtak et al. [5] used $N \sim 125,000$ galaxies from about 7,800 clusters from the Sloan Digital Sky Survey (SDSS), divided the galaxies into four bins according to their projected distances R from their respective BCGs, "stack" their light-of-sight velocities relative to their BCGs, carefully removed interlopers, and finally computed the mean velocity in each bin. In this paper, we investigate the pros and cons of the gravitational redshift approach, and for the first time introduce a new effect in galaxy clusters.

In fact, the gravitational redshift is supplemented by an additional redshift of comparable amplitude. For any metric theory of gravity [1] the space time near a galaxy cluster is described by the metric $d\tau^2 = (1 + 2\Phi/c^2)dt^2 - (1 + z)^{-2}(1 + 2\Psi/c^2)dx^2$. Light emitted from a cluster at redshift z is time-dilated with the ratio of the observed wavelength to the emitted wavelength satisfying:

$$\frac{c}{(1+z)} \frac{\lambda_{\text{obs}}}{\lambda_{\text{emit}}} = \left[c + \frac{\Phi - \mathbf{v}^2/2}{c} \right], \quad (2)$$

which reveals an additional effective radial velocity shift

$$\Delta_{\text{TD}} = [\langle |\mathbf{v}|^2 \rangle - |\mathbf{v}_{\text{BCG}}|^2]/2c, \quad (3)$$

owing to the transverse Doppler (TD) effect from random motions of galaxies in special relativity (SR).

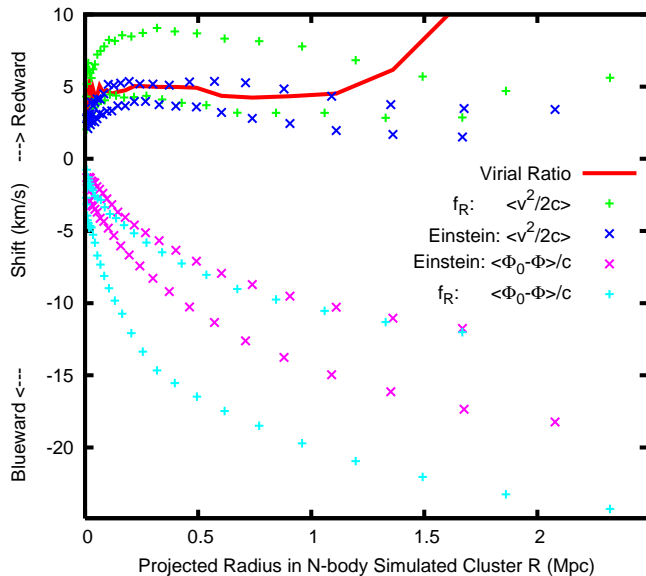


FIG. 1: Shows N-body simulations predicted TD and GR velocity shifts at projected radius R , annotated by $\langle v^2/2c \rangle$ and $\langle \Phi(0) - \Phi(r) \rangle / c$. **Pluses** show the 20th and the 1st biggest haloes of $r_{\text{vir}} = 1.67$ and 2.32 Mpc in $f(R)$ with $|f_{R0}| = 10^{-4}$. **Crosses** show the 10th and the 1st biggest haloes of $r_{\text{vir}} = 1.67$ and 2.08 Mpc in Einsteinian gravity. **The red thick line** shows the *dimensionless* virial ratio $\langle v^2 \rangle / \langle Z \partial_Z \Phi \rangle$ for typical halos in GR, which deviates from its equilibrium value 3, especially at larger radii, i.e., the TD effect is 1 to 4 times its equilibrium prediction.

Wojtak et al. [5] reported a blueshifting of the mean apparent line-of-sight velocity of the galaxies in the SDSS clusters, again relative to the BCG, which was then interpreted as purely GR. But this interpretation is incomplete. The TD effect always co-exists in proportion to GR because of the Virial Theorem:

$$\langle -\Phi/2 \rangle / 2c = \langle GM/r \rangle / 2c = \langle |\mathbf{v}|^2 \rangle / 2c, \quad (4)$$

where M is the mass enclosed within a radius r , $\langle \rangle$ denotes the averaging over all gravitational masses in the whole virialized volume of a cluster, and the factor of $1/2$ in front of Φ prevents double counting of the pairwise mutual potential. Thus the random kinetic energy per unit mass $\overline{\mathbf{v}^2}/2$ is globally 25% of the average potential $-\overline{\Phi}$. The ratio of $1/4$ holds even after averaging over a distribution of clusters of different mass and for clusters of any density profile and anisotropy parameter, so the Virial Theorem is a robust link between TD and GR effects, and their superposition is observed as the mean velocity shift. **In Fig 1. we show the TD and GR shifts in haloes from the N-body simulations of [3]. As we can see that haloes tend to be blue-shifted at large radii compared to their centres due to combination of GR and TD effects. In reality, however, Fig. 1 shows that the TD effects are often enhanced by a factor 1 to 4 in halos in N-body simulations because their virial ratio often deviates from the expected value at virial equilibrium.**

It seems straightforward to test many gravity theories with their gravitational redshift prediction. However, **recent tests of modified gravity often assume that clusters have dark halos**, which complicates the tests. E.g., **Hu & Sawicki [6] show in $f(R)$ gravity with $|f_{R0}| = 10^{-4}$ the Newton constant G is boosted by a nearly constant factor $4/3 \simeq 1.33$ for typical halos on cluster scales.** For a fixed cluster mass Wojtak et al. claimed that this 33% boost of the gravitational redshift signal robustly distinguishes Modified Gravity from Einsteinian Gravity. Such a claim, however, has a flaw: the total mass of the dark halo is an unknown free parameter, which must be determined by fitting the observed velocity dispersion as a function of distance from the cluster centre. Since G appears only in the combination GM , one can cancel essentially the enhancement of G in $f(R)$ gravity by reducing the halo mass parameter M , thus obtaining the *indistinguishable* fit to the velocity dispersion curve and to the mean velocity shift signal. **Nevertheless, one could test whether statistics of redshift data and halo counts is indeed biased towards more massive haloes, as generically found in $f(R)$ theory. Fig. 1 shows very massive haloes are more frequent in $f(R)$ gravity than in Einsteinian gravity, but for haloes of similar virial radius or virial velocity or GM_{vir} , two theories predict a similar shift.**

A more specific example is to use the isotropic Jeans equation $-GM/r^2 = d(n\sigma^2)/n dr$, where the tracers, i.e., galaxies are assumed an isotropic dispersion $\sigma(r)$ and a number density $n \propto r^{-\gamma}$ at large radius r . One solves for the

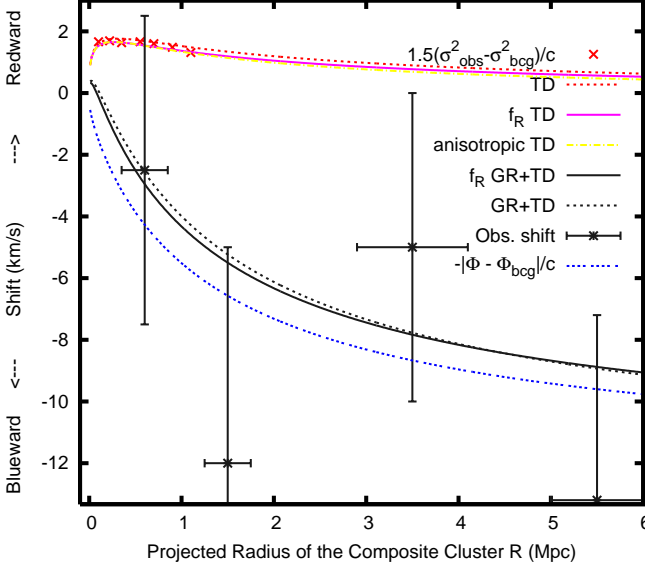


FIG. 2: Shows consistency of the data (crosses and error bars) [5] with the competing GR effect $-\overline{[\Phi - \Phi_{\text{BCG}}]}/c$ plus TD effect $(\overline{v^2} - v_{\text{BCG}}^2)/2c$; the 3D kinetic energy $\overline{v^2}/2$ at any R equals $QZ\overline{\partial\Phi/\partial Z}$ averaged over the line of sight depth z , where $Q = 3/2$ within the virial radius r_{vir} of an isotropic cluster, except $Q \simeq (3r_{\text{vir}} + r)/(2r_{\text{vir}} + r)$ for the yellow line to mimic mild anisotropy and non-equilibrium at large radii. Clusters are all modelled as NFW haloes, weighted by $M_{\text{vir}}^{-7/3}$ in the virial mass range $M_{\text{vir}} = (0.11 - 2) \times 10^{15} M_{\odot}$ in Einsteinian gravity (dashed), or $M_{\text{vir}} = (0.09 - 1) \times 10^{15} M_{\odot}$ in $|f_{R0}| = 10^{-4}$ gravity (solid) with a 33% boost of the effective G in these lightish haloes (Fig. 3 of [8]).

random kinetic energy $\overline{v^2}/2 = 1.5\sigma^2 = (1.5GM/r)/(\gamma + 1)$, which is locally $\simeq 3/8 - 3/10$ of a Keplerian potential GM/r for a galaxy count profile with $\gamma \simeq 3 - 4$ at large radii. The ratio $3/8$ or $3/10$ holds even after stacking of clusters of different masses and line-of-sight projection. This argument is true in standard gravity as well as in $f(R)$ gravity. Clearly gravity models with the same GM predict the same dispersion curve, and velocity shifts.

To compute the TD and GR effects generally at any projected radius, we start with the isotropic Jeans equation $-\partial(n\sigma^2)/\partial Z = n\partial\Phi/\partial Z$ for the observable tracers (galaxies) with a number density $n(r)$ in equilibrium in the potential $\Phi(r)$. We integrate this over the line-of-sight depth Z through a cluster after multiplying by ZdZ , and apply an integration by parts to $Zd(n\sigma^2)$ to drop the total derivative term. We find $\int_{-\infty}^{\infty} dZ (n\sigma^2) = \int_{-\infty}^{\infty} dZ (nZ\partial\Phi/\partial Z)$, which predicts that inside the virial radius the specific 3D kinetic energy averaged in a projected annulus R to $R+dR$ is $\langle |v|^2 \rangle / 2 = \langle GM(r)QZ^2/r^3 \rangle$, where $Q = 3/2$ from quadrature sum of the three velocity components. This expression allows us to predict the SR effect at all radii for any matter density in any metric-based gravity theory, since the Jeans equation applies to any force which is a gradient of a potential. E.g., if the density is $\sim r^{-\gamma} \sim r^{-3}$ and gravity $\sim r^{-2}$ then $\langle v^2 \rangle / 2 = (3/8) \langle |\Phi| \rangle$, where $\langle |\Phi| \rangle = (\pi GM/4R)$ is the density-weighted line-of-sight integration of $|\Phi|$.

To compute the GR and TD effects for the SDSS clusters, we account for different cluster masses using a Salpeter-like mass function $dN/dM_{\text{vir}} \sim M_{\text{vir}}^{-2.33} \sim M_{\text{vir}}^{-7/3}$ between the mass range M_l and M_u as Wojtak et al., so

$$\langle |v|^2 / 2 \rangle = \overline{(QZ^2/r)(d\Phi/dr)} / \overline{1}, \quad \langle \Phi_0 - \Phi \rangle = \overline{(\Phi_0 - \Phi(r))} / \overline{1}, \quad \overline{A} \equiv \int_{M_l}^{M_u} dM_{\text{vir}} \int_{-\infty}^{\infty} dZ n(r) A|_{r=\sqrt{Z^2+R^2}}, \quad (5)$$

where \overline{A} is essentially a stacked density-weighted line-of-sight integration of a quantity A at the projected radius R , and the spherical potential and tracer (galaxy) number count density are given by $\Phi(r) = -\frac{GM_{\text{vir}}}{rF(C)} \ln(1 + rC/r_{\text{vir}})$, and $n(r) \propto \frac{M_{\text{vir}}^{-7/3}}{4\pi F(C)} \frac{N_{\text{vir}}}{r(r+r_{\text{vir}}/C)^2}$, where $F(x) \equiv [\ln(1+x) - x/(1+x)]$. We fix the halo concentration parameter $C = 5$ and the virial radius $r_{\text{vir}} = 1.2 (M_{\text{vir}}/10^{14} M_{\odot})^{1/3}$, as determined in [5]. Such a spherical NFW potential is an approximation to the true potential in Einsteinian gravity; in $f(R)$ gravity the potential from N-body simulations tends to be more concentrated [3] and in TeVeS gravity the potential tends to have a pure $\ln(r)$ profile at large radii. A reasonable analytical approximation of the tracer (galaxy) count $n(r)$ is the spherical NFW profile with the count of galaxies inside the virial radius $N_{\text{vir}} \propto M_{\text{vir}}$. Here we do not attempt to model the detailed selection criteria of galaxies of measurable redshift and the off-centredness of the BCGs since these complexities seem

not to be the fundamental issue here. We do model the effects of mild anisotropy and non-equilibrium at large radii. From N-body simulations of [3, 9] we find that $Q \simeq (3r_{\text{vir}} + r)/(2r_{\text{vir}} + r) \leq 3/2$ works well empirically.

The results for Einsteinian gravity are shown in Fig. 2 for a halo mass range of $(M_l, M_u) = (0.11 \times 10^{15}, 2 \times 10^{15})M_\odot$. Note these fitting parameters are deduced from hydrostatic balancing of the pressure gradient $d(n\sigma_{\text{obs}}^2)/(n dr)$ and the halo gravity, as one cannot directly observe the halo and measure its mass. One can see our choice of parameters can fit the observed $(3\sigma_{\text{obs}}^2 - 3\sigma_{\text{BCG}}^2)/2c$ curve of [5] and, in doing so, we can predict the $-|\Phi(R) - \Phi_{\text{BCG}}^2|/c$ GR curve. Note the inevitable *reversal* from the observed average $\simeq 6.5 \pm 4 \text{ km s}^{-1}$ blueshifting to redshifting when within 0.2 Mpc of the BCG (cf. grey error bars and lines in Fig. 2) due to TD: the line-of-sight dispersion of non-BCGs $\sigma_{\text{obs}}(R) \simeq 600 \text{ km s}^{-1} \simeq 3\sigma_{\text{BCG}}$ converts directly to a $(3\sigma_{\text{obs}}^2 - 3\sigma_{\text{BCG}}^2)/2c \simeq 1.6 \text{ km s}^{-1}$ TD differential redshift near an isotropic cluster centre. The TD signal (red crosses) is clearly both non-negligible and model-insensitive, and is thus a robust constraint applicable to any metric-based gravity theory.

As stated earlier, one should not compare an $f(R)$ gravity model with an Einsteinian gravity model of the same halo mass distribution, namely $(M_l, M_u) = (0.11 \times 10^{15}, 2 \times 10^{15})M_\odot$, since it would overpredict the velocity dispersion curve $\sigma^2(R)$ everywhere by the same factor of 4/3, which can be ruled out without even measuring gravitational redshift. In fact the isotropic Jeans equation ensures a **one-to-one** relation between the SR and GR effects. The mass distribution where all (halo virial) mass is lowered by the same factor 4/3 would predict a velocity dispersion curve identical as the Einsteinian curve. Instead, to show some difference, here we adopt $(M_l, M_u) = (0.09 \times 10^{15}, 1 \times 10^{15})M_\odot$, and the result is shown as solid lines in Fig. 2. This $f(R)$ model produces GR and TD shifts by amounts essentially identical to Einsteinian gravity. Thus GR, TD and the velocity dispersion profile contain essentially three redundant copies of information about a metric theory, up to some uncertainty from anisotropy.

Likewise, the claimed $(0-10) \text{ km s}^{-1}$ extra shift in TeVeS reduces to only $(0-3) \text{ km s}^{-1}$ when adopting mass models consistent with σ_{obs}^2 [7]. Unfortunately the TD effect is left out explicitly in *all* these papers: e.g., TeVeS predicts a roughly radius-independent SR red-ward shift of $\langle (3Z/2c)\partial\Phi(r)/\partial Z \rangle = 3\sigma_\infty^2/\gamma c \simeq 1 \text{ km s}^{-1}$ for $\gamma \sim 3$. Further investigation including all relativistic effects in $f(R)$ N-body halo simulations [3, 8] would be needed.

While we cannot break degeneracy of gravity theory as long as different effective G and halo mass M yield the same virial velocity, the differential shift in a cluster is a **remarkably sensitive** measure of the mass function of haloes within the standard gravity. It can be easily shown that, the global gravitational shift with respect to the center, integrated inside **an aperture of $R \rightarrow \infty$** and averaged over all haloes, is given by

$$\langle c\Delta_{GR} \rangle \equiv \frac{\int V_{\text{vir}}^2 dN}{\int dN} \langle f \rangle = \frac{(3\alpha - 3)[1 - (V_{\text{vir},l}/V_{\text{vir},u})^{3\alpha-5}]V_{\text{vir},u}^2}{(3\alpha - 5)[1 - (V_{\text{vir},l}/V_{\text{vir},u})^{3\alpha-3}]} \frac{C}{F(C)}, \quad (6)$$

where $f(r) \equiv \frac{\Phi(0) - \Phi(r)}{V_{\text{vir}}^2} = [-1 + \frac{r_s}{r} \ln(1 + \frac{r}{r_s})] \frac{C}{F(C)}$ is a rescaled NFW potential, $\langle f \rangle = \frac{C}{F(C)} \sim 5$ is its density weighted global average for halos of typical concentration $C \sim 5$. Here the mass function $dN \sim M_{\text{vir}}^{-\alpha} dM_{\text{vir}} \sim V_{\text{vir}}^{-3\alpha+2} dV_{\text{vir}}$ for the virial velocity between the lower bound $V_{\text{vir},l}$ and upper bound $V_{\text{vir},u}$. For a fixed power-law index $\alpha \sim 7/3$, the differential shift $\langle c\Delta_{GR} \rangle \sim 10V_{\text{vir},u}^2$, which is an indirect measurement of the virial velocity $V_{\text{vir},u}$ at upper mass cutoff.

Note finally the future possibility of other relativistic effects[4], e.g., measuring the GR and TD effects from cluster X-ray gas spectra. This has less need for stacking clusters because of negligible σ/\sqrt{N} uncertainty for the countless ionized gas particles. The signal also differs from the technique of [5] because the X-ray gas particles have a profile different from that of galaxy number density, and less velocity anisotropy than galaxies. By comparing the transverse Doppler signals of different tracers one could even infer the velocity anisotropy of galaxies inside clusters.

-
- [1] Peacock J. A. *Cosmological Physics CUP* (1999); Angus G. *et al. ApJ* **654** L13 (2007); Gentile G *et al. Nature* **461**, 627 (2009); Gentile G. *et al. Astron. & Astrophys.* **472** L25 (2007); Galianni P., *et al. PRD* **86**, 044002 (2012);
[2] Li B. *et al. MNRAS* **421** 3481 (2012); Zhao H. *et al. ApJ* **712** L179 (2010);
[3] Zhao G., Li B., Koyama K. *Phys. Rev. Lett.* **107** 071303 (2011); *Phys. Rev. D* **83**, 044007 (2011)
[4] Lopresto J.C., Schrader C., Pierce A.K., 1991, *ApJ*, **376**, 757; Skibba R. *et al.*, 2011, *MNRAS*, **410**, 417, Kim Y.-A., Croft R. 2004, *ApJ*, **607**, 164.; Broadhurst T., Scannapieco E., *ApJ*, **533**, L93 (2000); Kaiser N., 2013, arXiv1303.3663
[5] Wojtak R., Hansen S.H., Hjorth J. *Nature* **477**, 567 (2011)
[6] Hu W., Sawicki I., *Phys. Rev. D* **76**, 064004 (2007)
[7] Bekenstein J. D. , Sanders R.H., *MNRAS* **421**, L59 (2012)
[8] Schmidt F. *Phys. Rev. D* **81**, 103002 (2010)
[9] Maccio A., Mirante G., Bonometto S.P. *ApJ* **588**, 35-49 (2003)